

# Numerical modelling of the seismic response of gas pipelines in liquefiable sand

*Márkosz Topalidisz*

t.markosz@gmail.com

Instituto Superior Técnico, Universidade de Lisboa, Portugal

July 2018

---

## Abstract

The numerical simulation of liquefaction is a highly nonlinear problem. Due to these facts predicting the effect of soil liquefaction is extremely difficult. The aim of this thesis is to investigate the effect of a cyclic loading and liquefaction on underground circular gas pipelines. The numerical analysis was made in the finite difference software, FLAC 2D.

The first part focuses on understanding the modelling concepts necessary to provide an accurate model to describe the phenomenon. Such concepts are the mechanism of the nonlinear-elastic constitutive model invoked by hysteretic damping, pore water pressure generation, shear wave propagation in 1D condition. Then, different lateral boundary conditions are put into comparison, namely free-field boundary condition and tied node boundary condition with attach command or with rigid beam.

Secondly, the behaviour of a gas pipeline in a liquefiable sand layer was studied. The influence of the phenomenon of the pipeline in terms of horizontal, vertical displacements and evolution in stresses are shown.

---

Keywords: **liquefaction, earthquake, pipeline, numerical modelling, FLAC.**

---

## 1. INTRODUCTION

Liquefaction is a highly complex phenomenon and produces devastating effect during earthquake.

The building codes in many countries require engineers to consider the effects of soil liquefaction in the design of new buildings and infrastructure such as bridges, embankment dams and retaining structures. But the high complexity of the phenomenon makes for these building codes really hard to estimate the real behaviour of the soil and the response of the structure, therefore for detailed investigations numerical analysis is made.

As one of the biggest energy resource, natural gas is used, which are transferred through pipelines inside the soil. Since the damage of the pipelines would consequent in a highly dangerous outcome, and also since in Portugal there is a high risk of an earthquake occurrence, it is important to investigate the effect of liquefaction on these structural elements.

The scope of the thesis to investigate the effect of liquefaction with FLAC, a finite difference

software, providing an accurate numerical analysis to discover the problem.

First, a single element was investigated, in order to find out the extends and limitations of the linear and nonlinear elastic-perfect plastic constitutive model. This is followed by introducing pore water pressure generation, thus liquefaction to the element.

After a 1D model was used to study shear wave propagation and pore water pressure generation.

Also, in this section great effort was made to identify the most suitable boundary conditions which describes the phenomenon most accurately.

2D model was made with and without the pipeline. It was intended to find out how the tube is influenced in terms of stresses and displacements due liquefaction.

Finally, the conclusions are made considering the results gained through the work.

## 2. SIMPLE ELEMENT: LINEAR-ELASTIC VS. NONLINEAR ELASTIC

In this section a single-element analysis was made to show the main features of model response. Firstly, the extends and limitation of the linear elastic-perfectly plastic constitutive model was studied. Then, by adding nonlinearity to the elastic part, a better, strain dependent representation of the stiffness and damping degradation curves was achieved.

As a motion a harmonic acceleration-time history was used, with increasing amplitude (1,2,4,8,16,32) over time, and the soil properties shown in Table 1 were adopted:

**Table 1. Soil parameters: single element**

$\gamma$ [kN/m <sup>3</sup> ]	E [Mpa]	$\nu$ [-]	G [MPa]	$V_s$ [m/s]	$c'$ [kPa]
20	20	0,2	8,3	64,6	20

It can be seen, that the cohesion of 20 kPa defines the strength of the material. Plastic behaviour is expected, when  $\tau=20$ kPa is reached, regardless of the confining pressure.

During the verification first, a linear elastic-perfectly plastic constitutive model, with Mohr Coulomb failure criteria was investigated. Until amplitude 16, the model stays in linear elastic range. On the other hand, when the amplitude is increased to 32, the model is reaching the plastic plateau as it was expected.

FLAC provides a built-in model, which supplement the linear-elastic perfect plastic model and provides a nonlinear elastic behaviour. Therefore, the yield surface is still defined by the Mohr-Coulomb failure criterium, with no hardening.

This is developed by creating an S-shaped modulus reduction curve by a cubic equation, with zero slope at both low and high strain. To obtain such a curve in FLAC, these logarithmic strain levels, namely  $L_1$  and  $L_2$  has to be defined.

Apart from hysteretic damping, also a small amount of Rayleigh-damping was adopted, since at low level cyclic strain levels there is almost no energy dissipation during hysteretic damping, which is unrealistic.

For this model 2% of Rayleigh damping was adopted, at the fundamental frequency of the soil element, which is 16 Hz.

Figure 1 shows the effect of damping, the dissipated energy which corresponds to the area of each cycle, which was zero in the previous case. Also, the degradation in stiffness can be seen, since the secant modulus of each cycle is decreasing with the increase of amplitude, therefore with the increase of strain level.

Unlike the previous case, when the amplitude is set to 32, it can be seen, that due to the energy dissipation, the response does not reach the 20kPa threshold value. The obtained strains are considerably higher, than before, but despite the deceiving strain level, the perfect-plastic state had been not reached, according to the constitutive model.

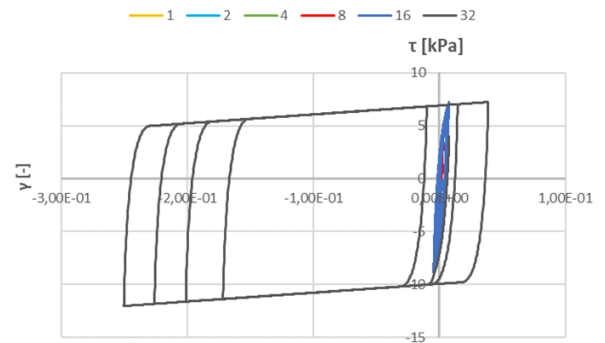


**Figure 1. Stress strain curves in plastic region: nonlinear elastic-perfectly plastic model (Amplitude of the motion: 1; 2; 4; 8; 16; 32)**

Finally from the FLAC results, comparison was made against the model's theoretical stiffness degradation curve. Note has to be taken, that the theoretical curve was adjusted by a stiffness-degradation curve obtained by the Ishibashi& Zhang (1993) correlation.

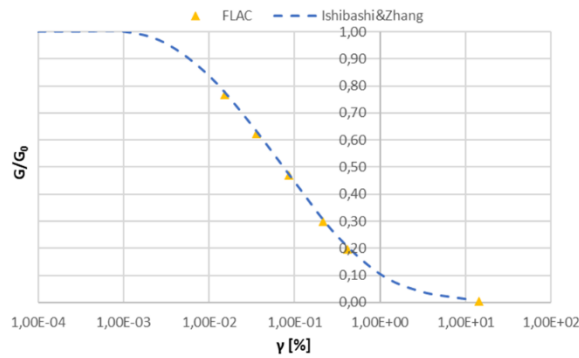


Figure 2. Stiffness degradation curve obtained by the Ishibashi& Zhang correlation in comparison with FLAC results

Figure 2 shows a good match between theoretical approach and FLAC results.

### 3. SIMPLE ELEMENT: SIMULATION OF PORE WATER PRESSURE BUILD-UP

In order to simulate the generation of pore water pressure, the FLAC's built in "Finn" constitutive model was used, which can be activated together with the non-linear elastic model with Mohr-Coulomb failure criterion.

As the main aspect of liquefaction is related to undrained response, the Finn model computes the variation in volume, using the equation proposed by Martin (1970) and Byrne (1991).

$$\frac{\Delta \varepsilon_{vd}}{\gamma} = C_1 \cdot \exp\left(-C_2 \left(\frac{\varepsilon_{vd}}{\gamma}\right)\right) \quad (1)$$

Where:

- $\Delta \varepsilon_{vd}$ : variation of volume
- $\varepsilon_{vd}$ : accumulated irrecoverable volume strain
- $\gamma$ : cyclic shear-strain amplitude
- $C_1$ : constant
- $C_2$ : constant, which usually takes the value of  $\frac{0,4}{C_1}$

Knowing the variation of volume, the model correlates it with the pore water pressure and mean effective stress the following way:

$$\Delta \sigma_m + \alpha \cdot \Delta p = K(\Delta \varepsilon + \Delta \varepsilon_{vd}) \quad (2)$$

Where:

- $\sigma_m$ : mean total stress
- $\alpha$ : Biot coefficient (=1 for saturated soils)

- $p$ : pore water pressure
- $K$ : drained bulk modulus
- $\varepsilon$ : volumetric strain increment

In terms of representation, the model stores the maximum value of the pore water pressure during the motion and updates it at each stress reversal. It results a stepping evolution, with straight jumps at the stress reversals.

During the model a single element was taken into consideration with a harmonic motion applied on it at the horizontal direction, simulating a simple shear test. Initial confining pressure were defined as 50kPa with 10kPa pore pressure as a zone variable, which all together creates the 40 kPa effective confining pressure.

For the dynamic conditions the free field boundary condition was used, which are dashpots placed into the gridpoints, calculating also the pore water pressure generation.

The soil properties were taken, so it would represent a typical sand. For that the VELACS research study by Arulmoli et al. (1992) was taken as a reference.

#### 2. Table Soil properties: Single element- generation of pore water pressure

	$\gamma$ [kN/m <sup>3</sup> ]	G [Mpa]	K [MPa]	$c'$ [kPa]	$\phi$ [°]
Sand	15	44,64	116,41	0	35
	L1 [-]	L2 [-]	C1 [-]	C2 [-]	
Sand	3,00	0,80	0,8	0,5	

The amplitude of the shear stress was set to 2,25kPa, which defines a CSR=5,625%

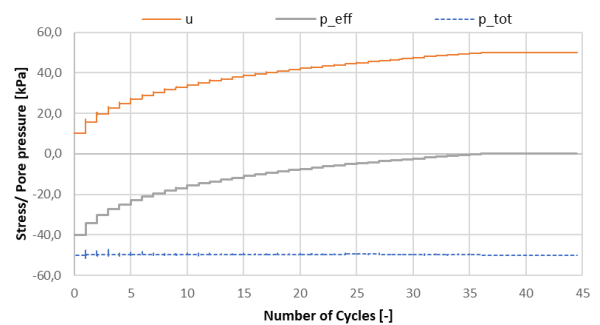


Figure 3. Stress and Pore water pressure evolution, CSR=5,625%

In Figure 3 the pore water pressure (u), mean total stress (p\_tot), and mean effective stress (p\_eff)

evolution is represented. It shows how the pore pressure rises, and the effective stress decreases to zero due to the repeated set of cyclic motion. This happens in a form of straight jumps, when the sinusoid motion reaches its “positive” or “negative” peak, in other words when there is a stress reversal in the applied action. At that moment also, a new peak will appear in the generated pore water pressure, which is registered by definition by the Finn model. This phenomenon repeats itself until the effective earth pressure reaches the zero value. Then liquefaction occurs, and there will be no more pore water pressure generation. Since due to the boundary conditions the pore pressure was set to 10kPa and the effective confining pressure was 40kPa, the initial values are these values, which can be also observed in (Figure 3).

Although the liquefaction was reached properly in the model, it was observed, that at the stress reversals there are certain jumps appearing.

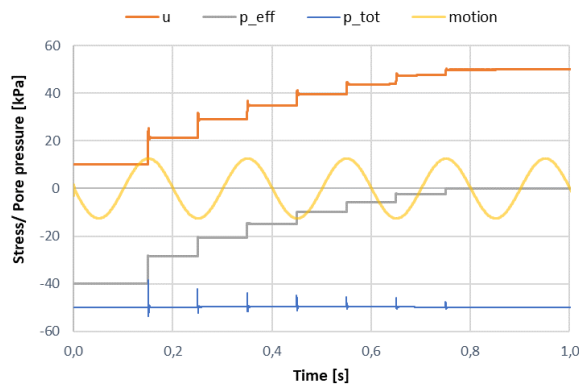


Figure 4. Representation of the jumps during stress and pore pressure evolution

Figure 4 shows that these jumps appearing at both the pore water pressure and total stress, but not at the effective stress evolution. The motion was also plotted in the figure, intended to show the harmonic nature of it, without any irregularity which could justify this phenomenon.

The jumps appear when the cyclic shear strain is updated after a stress reversal. At that instant, the pore water pressure rises, which is computed by the rise in total stress, as the formulation is written in total stresses (Eq.2). Then after a few calculation steps the equilibrium is reached again.

Since there is no explanation about this phenomenon in FLAC manual (2011) further investigations were made considering the effect of timestep, replacing free-field boundary conditions with fluid flow boundary condition, neglecting dynamic effects and the effect of Rayleigh damping. Studies has shown that the jumpings can be controlled with the Rayleigh damping, therefore the higher the damping is, the less significant will the jumpings become.

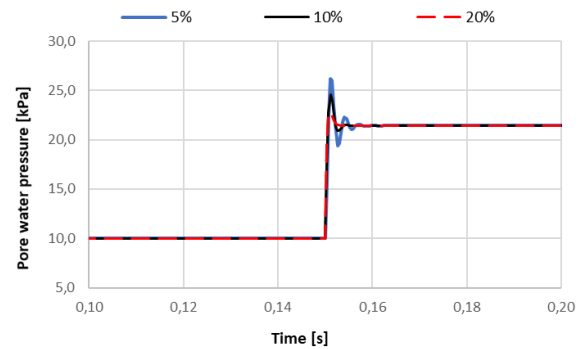


Figure 5. Difference in jumping due to increasing of Rayleigh damping

Following that, taking as a reference the cyclic liquefaction tests made within the scope of VELACS, and the relation according to Lee and Albaisa (1974) and DeAlba et al. (1975), a model verification was made. In order to be able to compare the results on the same scale, the  $r_u$  (excess pore water pressure ratio) values were used to express liquefaction, while the number of cycles  $N$  is normalized to the number of cycles to reach liquefaction,  $N_{liq}$ .

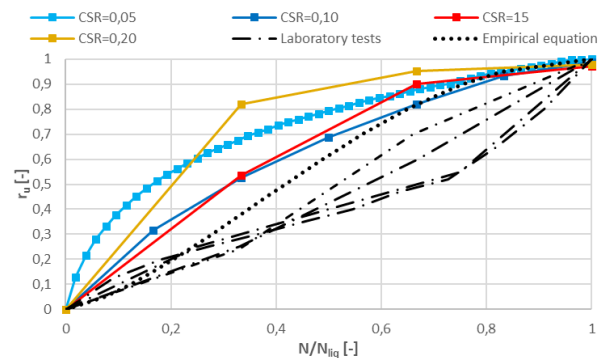


Figure 6. Comparison in the evolutions of excess pore water pressure ratio between results obtained in FLAC for different CSR values, laboratory tests and empirical equation

From Figure 6 it is visible that the model shows good agreement between experimental and simulated curves.

#### 4. 1D SHEAR WAVE PROPAGATION

Knowing the behaviour of a single element, the next step was to verify the accurate wave propagation in the model. That can be proven by providing a transfer function in the FLAC and compare it with the corresponding solutions. As the analytical solutions provide the shear wave propagation of the motion, the boundary conditions in FLAC were defined in a way, that displacements along vertical direction was restricted.

Dynamic boundary conditions have to be considered, in a way that wave propagation is not affected by the borders of the model continuum. At the bottom boundary of the model, it is achieved by the so called “Quiet-boundary”. The bottom boundary may be simulated as rigid boundary, which means, that there will be no energy dissipation, when the downward propagation waves reach it, they will be fully reflected. The Quiet-boundary condition introduces dashpots to each gridpoint on the applied border in both normal and shear direction, to simulate the wave dissipation.

As for the vertical boundaries the “Free-field” boundary condition is proposed by FLAC, which is yet again, dashpots placed along the gridpoints of the corresponding boundaries. The infinite medium is reached by connecting the main grid through the dashpots, to a free-field grid. The unbalanced forces from the free-field grid is applied to the main-grid boundary. It has to be mentioned, that the properties of these dashpots are corresponding to the initial properties of the soil. When large-strains are appearing (through liquefaction for example), there will be a significant degradation in stiffness, which the dashpots do not take into consideration. That can lead to unbalanced forces, that the model cannot handle properly, and leads to anomalies.

The acceleration (or velocity) time history of the motion is converted into stress according to the following equation:

$$\tau_s = -f \cdot \rho \cdot C_s \cdot v_s \quad (3)$$

Where:

- $\tau_s$ : applied shear stress
- $\rho$ : mass density
- $C_s$ : shear wave velocity
- $v_s$ : particle velocity at a given moment (velocity time history)

The term “f” in the equation stands for a factor, which considers the fact, that a major part of the input energy will be absorbed by the viscous boundary. Introducing the motion that way leads to a well-defined bottom-boundary condition.

Studies has shown, that if the Quiet-boundary dashpots are correlated to the properties of the bedrock, no further adjustment is needed, therefore  $f=1$  can be used.

The motion applied at the base was a harmonic acceleration-time history, with damping introduced in the motion, therefore the acceleration was monotonously decreasing over time. Because of elastic behaviour hysteretic damping was not introduced in the model, since there is no stiffness degradation considered. On the other hand, 2% of Rayleigh damping was adopted at 3,36 Hz.

The model was a 14m high 0,5m wide soil column, therefore providing the 1D conditions. At the bottom of the model an extra 0,2m were taken into consideration, with the rigid rock properties applied on it. It was necessary, so the dashpots from Quiet-boundary corresponds to the properties of the bedrock. The soil properties are shown in table 3.

**Table 3. Soil properties:1D shear wave propagations**

	$\gamma$ [kN/m <sup>3</sup> ]	E [Mpa]	G [MPa]	$\nu$ [-]	$V_s$ [m/s]
Soil	20,0	96,0	36,1	0,33	134,3
Bedrock	22,5	216,0	90,1	0,20	200,0

Comparison was made between the transfer functions obtained from DEEPSOIL and FLAC (Figure 7).

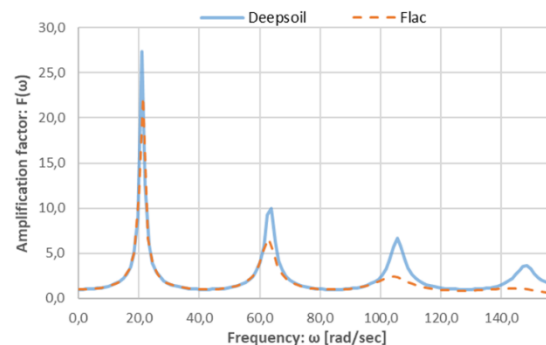


**Figure 7. Comparison in obtained transfer function using DEEPSOIL and FLAC**

It can be seen, that the two approach is fairly similar. Due to Rayleigh damping at the higher modes of frequencies there will be larger and

larger attenuation in the results obtained from FLAC.

### 5. WAVE PROPAGATION CONSIDERING PORE WATER PRESSURE GENERATION

The model was made based on the work of Bouckovalas et.al. (2016) which concluded a 1m wide, 14m high soil column, with 1x0,5m element size. There was no restriction defined except the movement in horizontal direction at the bottom (Figure 8).

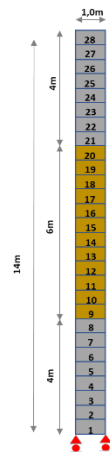


Figure 8. 1D model, with notation of the zone numbers

The soil properties for the 1D model were the following:

Table 4. Soil properties: 1D model with pore water pressure generation

	$\gamma$ [kN/m <sup>3</sup> ]	G [Mpa]	K [MPa]	$c'$ [kPa]	$\phi$ [°]
Top Clay	15	20,40	44,20	30	0
Nevada Sand	15	44,64	116,41	0	35
Bottom Clay	15	183,40	397,34	300	0
	L1 [-]	L2 [-]	C <sub>1</sub> [-]	C <sub>2</sub> [-]	C <sub>3</sub> [-]
Top Clay	-1,40	1,00	-	-	-
Nevada Sand	-3,00	0,80	0,8	0,5	0,0
Bottom Clay	-0,85	1,40	-	-	-

The applied motion was a harmonic acceleration, with the duration of 3sec. acting on the bottom of the model, with the amplitude of 3m/s<sup>2</sup>.

To model damping at low level cyclic strain level, Rayleigh damping was adopted to the model, which was tended to be adjusted to the natural frequency of the soil column.

FLAC has a built-in function to determine the fundamental-frequency by introducing a white noise input motion to derive the transfer function and, therefore the fundamental frequency. In terms of dynamic calculation FLAC proposes the use of free-field boundary condition in the lateral boundary of the models, where liquefaction was simulated, therefore it was intended to use it during the investigations.

During the investigations (Figure 9/left) it was observed that the deformed mesh shows differential displacements along the sides of the model. This is not satisfying the 1D modelling conditions.

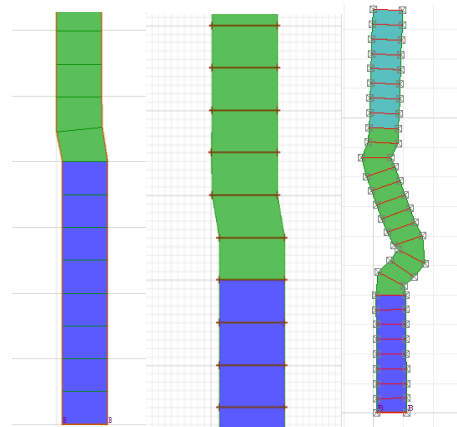


Figure 9. Deformed mesh: free-field boundary conditions (left) attached node (middle) tied-node with rigid beam(right)

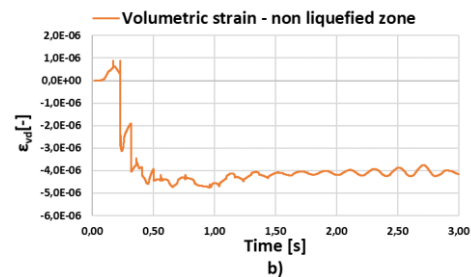
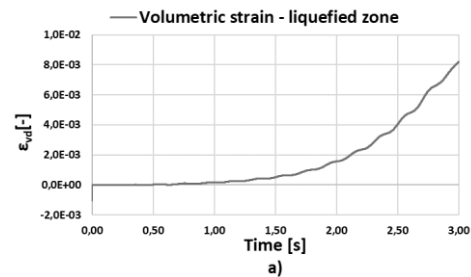


Figure 10. Volumetric strain evolution, using free field boundary condition in a) in liquefied zone, b) non-liquefied zone

In chapter 3, it was described that, the pore water pressure generation, as the evolution in mean total stress is governed by Eq. 2. Because of that, the volumetric strains were investigated in the liquefied zone (zone 9) and the zone above (Figure 10). FLAC defines compression as negative, extension as positive strain. Using Free-field boundary conditions (Figure 10 a)), the program predicts extension during liquefaction, which is not representative. Moreover, the volumetric strain is still increasing exponentially, even at the end of the calculation, it is not stabilising. Investigating the volumetric distortions in the same model, in the zone above, where liquefaction did not occur (Figure 10 b)), it is visible, that this case does not happen. Since due to the liquefied zone, a plastic hinge has developed, only a very small amount of acceleration is transmitted to the upper zones, which will cause just a little volumetric strain. But the phenomenon is still visible, that instead of extension, there is compression in the zone, as it should be.

It was mentioned before, that care has to be taken with the use of Free-field boundary condition, since the introduced dashpots are corresponding to the initial stiffness of the soil, which due to large deformations during liquefaction will degrade almost to zero. This will cause unbalanced forces, which will result in the phenomena presented above. At the liquefied zone the stiffness is highly degraded, so the force from the dashpots from the Free-field boundary condition will “squeeze” the zone from the sides, which will cause an increase in volume at the vertical side.

Knowing this, other approaches were investigated. First the tied-node boundary condition simulated with attached node command, that way defining, that the displacements at the two gridpoints in the opposite side should be the same.

The deformed mesh shows (Figure 9/middle) that there is no differential displacement along the two sides of the model, which satisfies the criteria of 1D model conditions.

The volumetric strain evolution also shows compression in the liquefied zone (Figure 11).

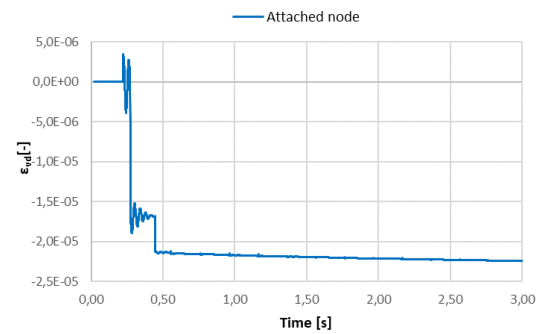


Figure 11. Volumetric strain evolution, using attached node boundary condition

An attempt was made for tied-node boundary condition simulated with horizontal beams, which connects the two nodes on the left and right side of the model. This way they restrain the horizontal movements at the two sides of the model to the same value.

The deformed mesh is visible in Figure 9/right. The beams connect the nodes in the two sides, but relative displacements between them allows the model to rotate, which is not acceptable in scope of 1D modelling.

For 2D investigations the attached node boundary condition was used.

## 6. SEISMIC RESPONSE OF GAS PIPELINES IN LIQUEFIABLE SAND

In this chapter, a 2D model was made. The model consisted a 15m high, 30m long soil continuum, with 0,5x0,5m elements. Three soil layers were taken into consideration, with the same properties, as during the 1D model. The upper clay layer was 2m thick, which was followed by a 6m thick sand layer, then the lower clay layer took place with 7m thickness. The upper and lower clay layer were addressed with non-linear elastic material model with Mohr-Coulomb failure criteria. The sand with the model, including the Finn model, to be possible the generation of pore water pressure. A pipeline with 0,8m diameter took place horizontally in the middle, with the centre 3m below the surface and with a uniform internal pressure equal to 80 bar applied inside to simulate the gas pressure. The element size around the pipeline was refined to 0,125x0,125m.

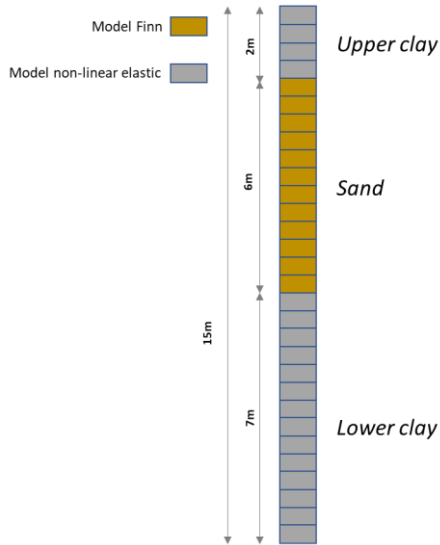


Figure 12. Detailed vertical profile in 2D model

Seeing the stress and pore water pressure evolution (Figure 13) at the liquefied zone, one can see, that the soil liquefies at around 2,3s, slightly before the strong part of the motion arrives. Until liquefaction occurs, as the pore pressure rises, the total stresses increase also, to achieving the isotropical stress state.

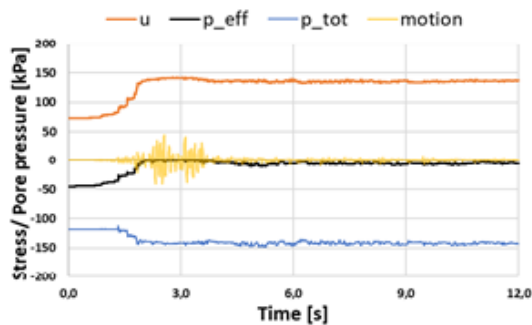


Figure 13. Stress and pore water pressure evolution in 2D model

Figure 14 shows the pore water pressure distribution in the model in the end of the analysis. A fairly uniform result is visible, compatible with the 1D response.



Figure 14. Pore water pressure distribution using attached node boundary condition

Until now structural element was not introduced to the model. The scope of the thesis was to study the effect of liquefaction on a gas pipeline. For practical reasons, in most of the cases the lowest (Figure 16 point A) and highest (Figure 16 point B) point of the pipe was taken into detailed investigation, since due to the refined mesh, the tube consists 32 liner elements. In order to impose, liquefaction will have an effect on the pipeline, initially the thickness of the sand layer was set to 3m, which is 2m below the centre of it (Figure 15).

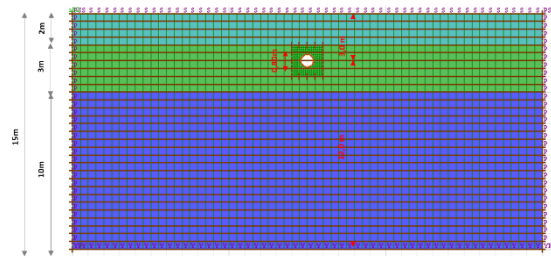


Figure 15. Initial geometry of the model

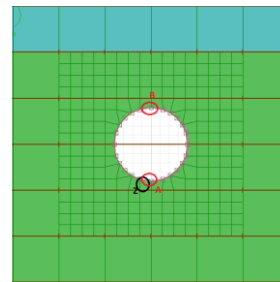


Figure 16. Detailed geometry around the pipeline, with marking the lower part of the tube (point A), upper part of the tube (point B) and the investigated zone below the pipeline (point Z)

Plotting the vertical (a)) and horizontal (b)) displacements it is visible, that the values at top and bottom are almost identical. This means that the pipe acts as a rigid body, and do not suffer deformations. The model did not predict failure in the pipeline, but care has to be taken. At “y” direction the displacements are not more than 0.5cm upwards, which shouldn’t cause significant damage. On the other hand, along the “x” axis the maximum displacement reaches the 7cm, which can cause failure in out of plain direction.

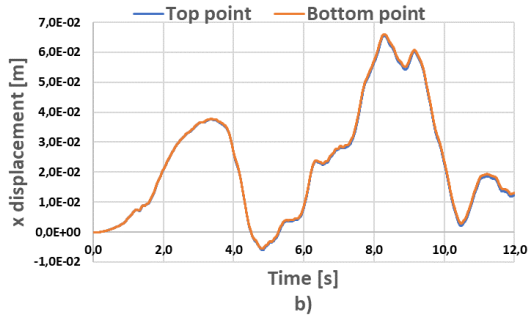
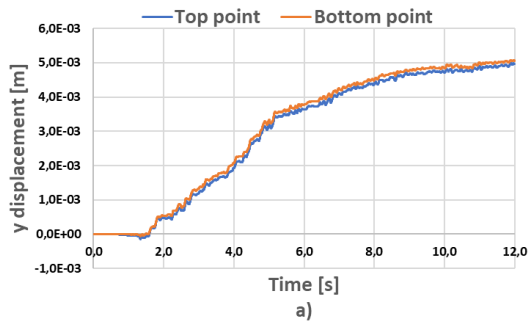


Figure 17. Vertical a) and horizontal b) displacements at Top (point B) and bottom (point A)

Plotting the vertical (a)) and horizontal (b)) displacements it is visible, that the values at top and bottom are almost identical. This means that the pipe acts as a rigid body, and do not suffer deformations. The model did not predict failure in the pipeline, but care has to be taken. At “y” direction the displacements are not more than 0.5cm upwards, which shouldn’t cause significant damage. On the other hand, along the “x” axis the maximum displacement reaches the 7cm, which can cause failure in out of plain direction.

But since at 2D conditions there are no deformations expected, the bending moment should reach a low value in respect of that.

As it is visible in Figure 18, there are indeed only a minimum amount of bending moments, which are even decreasing. Also checking the axial forces, one can admit, that it is almost constant, around 3130kN. One explanation for this phenomenon is that the 5mm steel and 0,8m diameter tube is stiff enough to sustain the loads, but more likely the applied pressure gives a high amount of additional stiffness, which will be more than enough to carry the weight of the soil. From the aspect of the load acting on the pipe, simplifying the situation and following the logic of just Newton’s second law, therefore:  $F=m \cdot a$ . Since the pipeline is installed close to the surface, the mass of the soil, which will act as an earth pressure, should be low. Also, when liquefaction occurs, there is a large amount

of attenuation in the motion. This reduces the acceleration, resulting in a lower amount of force acting on the structural element.

Summarising the investigations above, the pipe will act like a rigid body through the earthquake, without any significant stress generation inside the structural element, but due to the large amount of horizontal displacements it can reach failure in out of plane direction.

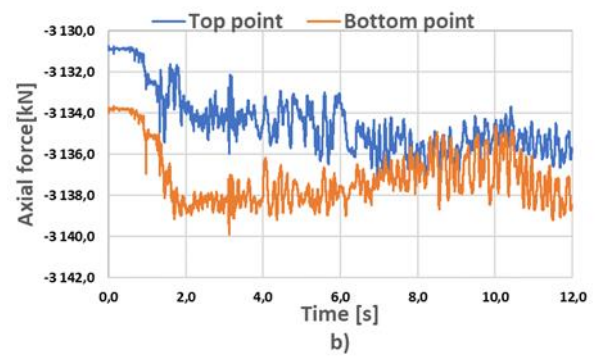
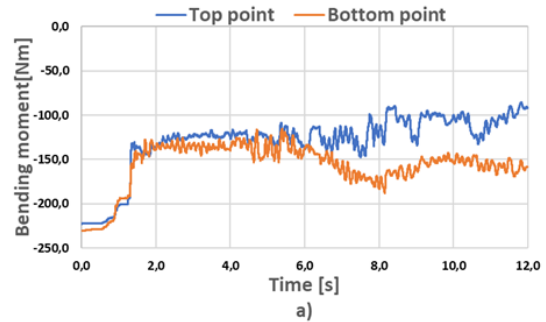


Figure 18. a) Bending moments and b) axial forces through time

Investigations were made by applying the Gilroy earthquake on the model, but with different scaling factor. It was intended to see, if the occurrence of liquefaction has effect on the horizontal displacements.

The scaling factors were the following: 0,001; 0,1; 0,5; 1,0; 1,5. alongside with Figure 19 shows the results.

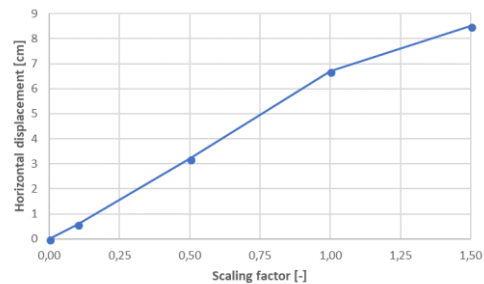


Figure 19. Results of horizontal displacements over increased scaling factor

At the beginning linear variation was predicted. But as liquefaction occurs, the motion is attenuated, therefore it was expected, that the slope of the line, thus the increase in horizontal displacements over scaling factor will be smaller. At 0,5 scaling factor liquefaction already occurs, but the slope of the line remains constant.

## 7. CONCLUSIONS

The scope of the thesis was to model and investigate the effect of liquefaction with FLAC on gas pipelines. First the nonlinear elastic-perfect plastic constitutive model was investigated on a single element. The main goal in this chapter was to show, that stiffness degradation in FLAC can be adjusted to a given, user defined stiffness degradation curve.

The pore water pressure generation through Finn model was investigated on a single element. Compared to laboratory tests, the model showed good agreement between experimental and simulated pore water pressure evolution. Also, it was discovered, that the jumps in the pore water pressure and effective stress evolution can be controlled by the Rayleigh damping.

Following that, a 1D model was investigated in terms of shear wave propagation. Studies has shown, that during the use of Quiet-boundary, if the Quiet-boundary dashpots are correlated to the properties of the bedrock, the multiplication factor can be neglected. The transfer-functions have been put into comparison between DEEPSOIL and FLAC. The two approaches shared fairly similar results, but note has to be taken, that as higher modes of vibrations are investigated, due to the Rayleigh damping FLAC predicts faster attenuation in transfer function.

To the 1D model pore water pressure was introduced. It was shown, that free-field boundary condition does not provide accurate solution. Therefore, other boundary conditions were investigated, such as tied node boundary condition simulated with either attached node command, or rigid beams and also attached node with free-field boundary condition combined. From these approaches, attached node and attached node with free-field boundary condition satisfied the 1D modelling conditions.

During the 2D modelling, first it was shown, that the use of attached node boundary condition provides fairly horizontal uniform result

compatible with the 1D response. Investigating the response of the pipeline, it was showed, that the internal pressure, the relatively small diameter and the 5mm thickness provides high stiffness to the structural element, therefore it moves as a rigid body. Also, there are neglectable bending moments arising through the motion. Note has to be taken, that due to the large horizontal displacements, failure can may occur along out of plane direction. When internal pressure is not present in the model, differential displacements becomes visible between the top and bottom point of the pipeline. This is proving the stiffening effect of the internal pressure. It was also observed, that the thickness of the sand layer has no effect on the axial forces and bending moment. Considering the horizontal displacements there was a decrease in the values over depth.

## 8. REFERENCES

- Arulmoli K., Muraleetharan K. K., Hossain M. M. e Fruth L. S. VELACS (1992): Verification of Liquefaction Analyses by Centrifuge Studies. Laboratory testing program – Soil data report. *The Earth Technology Corporation*
- Ishibashi I., and Zhang X. (1993): Unified dynamic shear moduli and damping ratios of sand and clay. *Soils and Foundations*, Vol. 33, No. 1, pp. 182-191
- Byrne, P. M. (1991): A Cyclic Shear-Volume Coupling and Pore-Pressure Model for Sand. *Second International Conference on Recent Advances in Geotechnical Earthquake Engineering and Soil Dynamics* (St. Louis, Missouri, March 1991), Paper No. 1.24, 47-55 pp.
- Martin G. R, W.D.L. Finn and H.B.Seed (1970): *Fundamentals of Liquefaction under Cyclic Loading*, J. Geotech., Div. ASCE, 101(GT5), 423-438 pp.
- Lee K.L. and Albaisa A. (1974): Earthquake induced settlements in saturated sands, *Journal of the Soil Mechanics and Foundation Division*, ASCE, Vol. 100, No. GT4
- DeAlba P., Chan C.K. and Seed H.B. (1975): Determination of soil liquefaction characteristics by large-scale laboratory tests, *Report EERC 75-14*, Earthquake Engineering Research Center, University of California, Berkley